Zeitschrift: IABSE reports of the working commissions = Rapports des commissions de travail AIPC = IVBH Berichte der Arbeitskommissionen

Band: 34 (1981)

Artikel: Non-linear finite element strategies for bridge slabs

Autor: Cope, R.J. / Rao, P.V.

DOI: https://doi.org/10.5169/seals-26895

Non-Linear Finite Element Strategies for Bridge Slabs

Stratégies pour l'analyse non-linéaire des dalles de pont à l'aide d'éléments finis

Nichtlineare Finite-Elemente-Strategien für Brückenplatten

R. J. COPE
Senior Lecturer

P. V. RAO
Research Fellow

Department of Civil Engineering, Liverpool University,
Liverpool, England.

SUMMARY
Bridge slabs have to carry repeated applications of heavy concentrated loading. Simple modelling strategies for realistic post-cracking analysis are presented with results from two element formulations. Acceleration techniques and criteria for establishing convergence are discussed.

RÉSUMÉ
Les dalles de pont doivent subir des applications réitérées de charges lourdes et concentrées. Ce rapport présente des stratégies simples qui mettent en modèle avec réalisme le comportement après fissuration et donne des résultats de deux configurations d'éléments. On discute les techniques d'accélération et les critères pour établir la convergence.

ZUSAMMENFASSUNG
Brückenplatten müssen wiederholte schwere und konzentrierte Lasten tragen. Über einfache Strategien, die das Verhalten im gerissenen Zustand realistisch modellieren, wird, zusammen mit Ergebnissen von zwei Elementenformulierungen, berichtet. Beschleunigungsmethoden und Konvergenzkriterien werden besprochen.

1. INTRODUCTION

The recent introduction of a limit state based design code in the U.K. [1] gives bridge engineers a choice in selection of analytical procedures. Use of non-linear methods would allow advantage to be taken of moment redistribution and 'membrane' action, but for such methods to become acceptable, they would have to be reliable and efficient. Non-linear finite element procedures show promise for a wide range of complex structural forms, not only as a primary analytical tool, but also for arriving at empirical design formulae.

High computing costs, specialised and sometimes subjective analytical techniques, at present associated with some finite element methods, are not appealing features. The expense of computing can be, to some extent, eased by selection of simple material models. However, modelling of the composite material has not advanced sufficiently for general section/element level force-displacement characteristics to be specified. The behaviour of the composite has to be built up from those of its constituents.

Non-linear analysis is performed by incremental, iterative procedures. By using acceleration schemes to expedite convergence, considerable savings can be made in computing costs. However, for objectivity of analysis, well behaved formulations have to be used and indices established to monitor convergence and degradation of stiffnesses. It is essential that analytical response is not distorted by the numerical procedure employed.

In this paper, finite element methods for bridge slab design are considered. Material models are described for predicting detailed load history and for use in design. Suitable indices for monitoring behaviour are established and a study of the BFGS acceleration procedure to reduce the number of iterations is reported. Unless stated otherwise, the analytical results presented were obtained using the Irons-Razzaque [2] general quadrilateral element. This is a non-conforming displacement model using numerical integration at 4 Gauss stations in plan and 5 integration stations through the depth [3]. Transverse shear strains are set to zero at the Gauss stations.

2. MATERIAL BEHAVIOUR MODELLING

Perfect bond is assumed between concrete and steel so a continuous strain field results over each element. Individual cracks are not represented, but 'smeared' over an area governed by the finite element mesh size. Flexural and in-plane stiffness components are obtained by superimposing concrete and steel effects. Concrete moduli are determined at the three-dimensional grid of integration stations. Steel reinforcement is represented by its axial stiffness in the correct direction and at the correct depth at the nearest Gauss station.

2.1 Concrete

Unstressed concrete is assumed to be isotropic. Although several multi-axial stress-strain relationships have been proposed for plain concrete, uniaxial values have been used. This is primarily because variations induced by fabrication and the limited accuracy of testing procedures, especially when prototype structures are concerned, make it difficult to justify a higher level of sophistication. A wide range of studies of slabs has shown that behaviour is relatively insensitive to the compressive stress-strain relationship used.

In the authors' approach, effective direct strains in the current principal strain directions are determined from:

$$\varepsilon_1^* = \frac{1}{1 - \upsilon^2} (\varepsilon_1 + \upsilon \varepsilon_2) \quad \text{and} \quad \varepsilon_2^* = \frac{1}{1 - \upsilon^2} (\upsilon \varepsilon_2 + \varepsilon_1) \qquad (1)$$

where $\varepsilon_{1,2}$ are the current principal strains and υ is Poisson's Ratio, which is assumed constant until cracking or crushing occurs, when it is set to zero. Compressive stresses are determined using a relationship proposed by Popovics, together with a plateau of constant strain between peak stress and a strain of 0.0035 [4]. Beyond that strain level, the stress drops to zero.

2.2 Composite Action

Most of the difficulties in simulating slab behaviour stem from the way reinforced concrete loses its tensile strength after cracking. In tension, a linear stress-strain relationship with a descending branch to simulate tension stiffening has been used with some success [4]. Much of the data on tension stiffening is based on studies of one-way bending, and the authors' tensile 'stress'-strain curve was designed to give good predictions of behaviour for a range of steel percentages [3]. The effectiveness of the model with cracks inclined to reinforcement cannot be gauged with confidence, because of the limited amount of experimental data available. Gilbert and Warner [5] have developed a tension stiffening model based on modifications to the stiffness of reinforcement. At the present time, there is a lack of generality in this approach and more work needs to be done to provide a basis for selection.

To follow repeated load application, an unloading curve parallel to the initial tangent has been found to give reasonable results [6]. However, for slabs that have been subjected to an unknown load history prior to analysis, best results are given when tension stiffening is ignored [6].

Two types of material model have been used. In the first, effective strains are determined in the current principal strain directions as described above. The effective stresses in these directions are obtained from the uniaxial relationship [4], and then resolved into Cartesian components for evaluation of mobilised internal resisting forces. With this approach, shear stress-strain is not modelled explicitly. Crack directions are only notional and they 'swing' in step with the current strain field.

In the second approach, material property axes are fixed in the prevailing principal strain directions at the end of iterations for the load increment in which cracking first occurs. The above uniaxial relationships are used in these directions, together with a constant in-plane shear modulus. Under subsequent loading, the principal strain directions can be significantly different to the directions of the material property axes. As a result, use of stress determination in fixed material property directions can result in poor predictions of behaviour, and the authors have used a strategy to rotate material property axes when intersecting crack patterns are present [4].

The changes in direction of principal values can be caused by a different load arrangement or can be due to internal redistribution of resisting forces. An indication of the magnitudes of swing in principal directions for a model skew slab bridge subjected to highway type loading can be seen in Table 1. Details of experimental and analytical studies of the slab, which was numbered 1A, are given in [6, 8]. The slab had a realistic steel arrangement with bars placed parallel and normal to the simply supported edges. The results presented are for a uniformly distributed loading equivalent to 1.2 times the self weight, and for monotonically increasing increments of 20kN. applied to a bogie of the design vehicle positioned as indicated in Fig. 1.

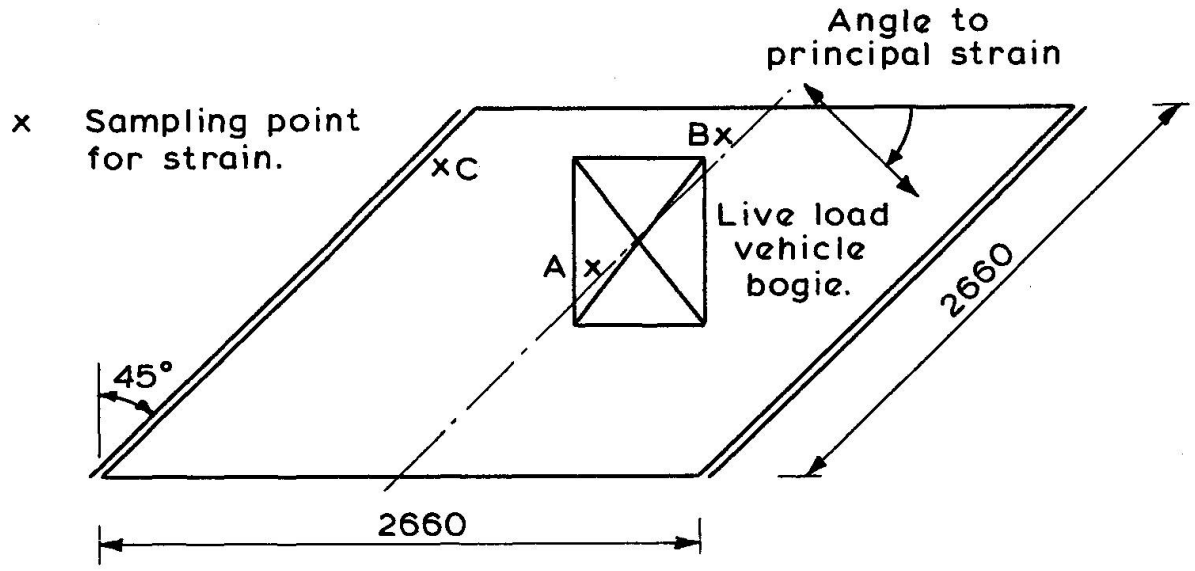

Fig. 1 Model Skew Slab

It can be seen that the principal strains are predicted to rotate considerably by the varying 'crack' direction method, whereas fixing the material property axes limits the rotation. The principal moments were obtained by integrating stresses through the depth at the Gauss stations and linearly interpolating to nodal points. Rotations of principal moments are less than those for strains, due to the influence of the reinforcement, and prior to yielding of steel there is a greater degree of agreement in their prediction. The large differences in principal angles for moments at C' and strains at C is due to the rapidly varying strain field in the obtuse corner.

Load	Linear Strain			Varying Crack Direction						Fixed Crack Direction					
				Strain			Moment			Strain			Moment		
	A	B	C	A	B	C	A'	B'	C'	A	B	C	A'	B'	C'
1.2xSelf Weight	38	20	72	37	19	73	40	27	112	37	19	73	40	27	112
+ 20kN.	35	15	79	33	11	88	44	36	115	34	16	89	44	32	111
+ 40kN.	34	13	81	29	7	89	46	34	114	34	15	90	46	28	109
+ 60kN.	33	12	82	28	2	90	44	33	107	34	14	90	42	24	104
+ 80kN.	32	12	82	28	1	92	44	32	112	33	14	91	42	20	107
+ 100kN.	32	11	83	22	- 1	93	43	29	108	32	14	91	39	20	109
+ 120kN.	31	11	83	21	- 4	94	43	28	108	32	14	91	39	19	103
+ 140kN	31	11	83	20	- 5	96	43	25	101	32	15	91	37	19	103
+ 150kN.	31	11	83	22	- 9	96	42	30	103	32	15	91	36	17	100
+ 160kN.	31	11	83	16	- 9	95	42	35	103	32	15	91	35	16	97
+ 170kN.	31	11	83	17	- 7	95	41	33	112	33	15	91	34	14	100

Table 1 Inclination of Principal Strain and Moment

Bazant [7] has commented on the inadmissibility of using orthotropic models because of their lack of directional invariance. He suggests that such models are reasonable when principal stresses do not rotate. The authors have found

that the 'varying crack direction' model gives the better overall comparison with experimental results [6, 8], and is satisfactory for design or assessment purposes.

3. MONITORING INDICES

Ideally, measurements of both equilibrium and displacement convergence are needed to terminate the iterative procedure at a given level of loading. Measures in common use depend on the differences between applied and mobilised resisting forces and iterative displacement vectors. Some of the norms presented in recent literature [3, 9, 10, 11] are examined to assess their suitability for use in analyses of concrete slabs.

For illustration, results from analyses of a reinforced concrete skewed slab (slab 2B of [6]) are discussed. The slab used is a one-fifth scale model and contains a realistic distribution of reinforcement. It is the most flexible of the slabs studied and thus presents the severest test for non-linear procedures. The analyses were performed using a 6x6 mesh [6], with a constant stiffness matrix, and no tension stiffening allowance for the concrete. Response values at four load levels with the design vehicle positioned as shown in Fig. 1, are presented for discussion. These cover response of the slab prior to yielding of the reinforcement.

3.1 Force and Displacement Norms

The authors have used two norms with consistent results [3]. A norm of out-of-balance loads in any direction (j) as defined by:

$$R_j = \frac{100 \times \sqrt{\Sigma (P_i - F_i)^2}}{\sqrt{\Sigma P_i^2}} \qquad (2)$$

where P_i is an applied nodal load, F_i is the corresponding internally mobilised force and the summations are taken over the global degrees of freedom in direction j. When there is no applied loading in a particular direction the denominator in (2) is set arbitrarily to 100, thus reducing R_j to a Euclidean norm. In this case it is not used to automatically control the number of iterations.

A norm of iterative displacements is defined as:

$$D_j = 100 \frac{(d_{j,max} - d_j)}{(d_{j,max})} \qquad (3)$$

where d_j is the Euclidean norm of the total displacement in direction j in the current iteration, and $d_{j,max}$ is the maximum d_j from previous iterations at the current load level. Experience has shown that satisfactory results are obtained when both norms are small in the transverse direction, but after yielding of reinforcement the number of iterations has to be limited when one of them is small.

Values of maximum displacement are compared in Fig. 2. The iterations at each load level were stopped when equilibrium and displacement norms of $R_3 = 2\%$ and $D_3 = 0.02\%$ were satisfied. There was some cracking on application of self weight, and although there was relatively little change in displacement, 31 iterations were needed to satisfy the equilibrium norm. This was due partly to

the unsymmetrical distribution of reinforcement about the slab's median plane. The addition of 20kN, via the idealised design vehicle, caused considerable cracking of concrete as evidenced by the big rise in deflection. 109 iterations were needed to satisfy the equilibrium norm. 72 iterations were needed for the next load increment of 20kN. With 60kN applied to the vehicle, a few bars behaved non-linearly and a maximum of 500 iterations were performed. At this stage, there was a 10% out-of-balance of equilibrium as measured by the norm R_3 and some of the implications of this are discussed below.

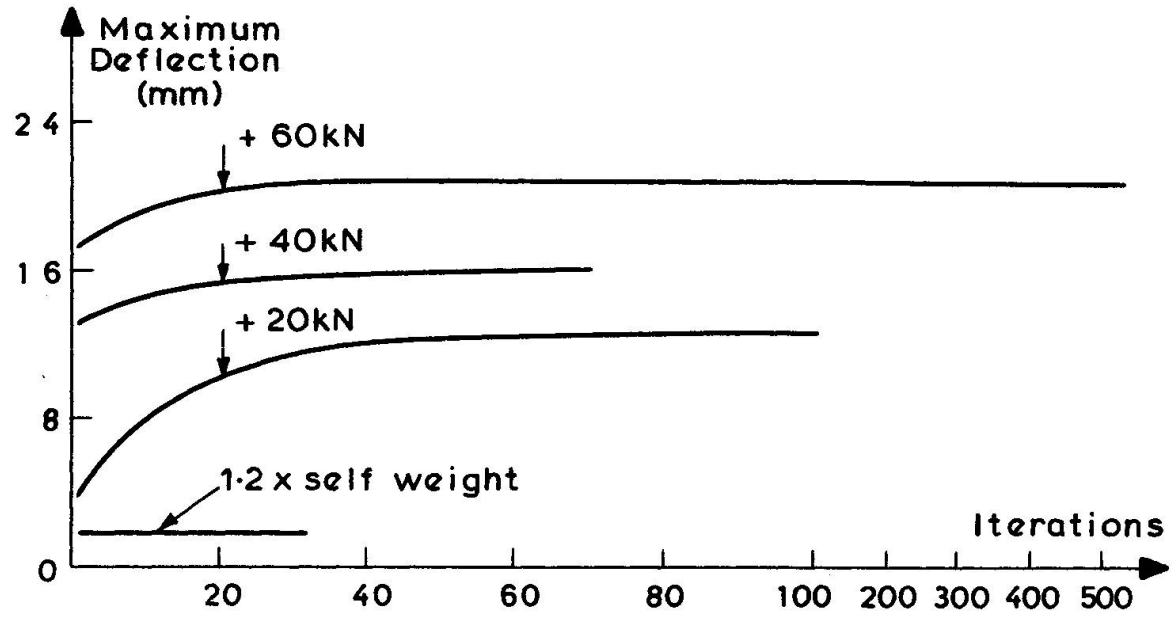

Fig. 2 Variation of Maximum Deflection

These results are typical for skew slabs, although the most flexible of the steel arrangements studied was selected to give the severest test of the procedure. At these load intensities, the biggest release of energy is in the first iteration. The rate of displacement convergence is very small after about 30 iterations and slabs reach an approximately steady state without equilibrium norms being satisfied.

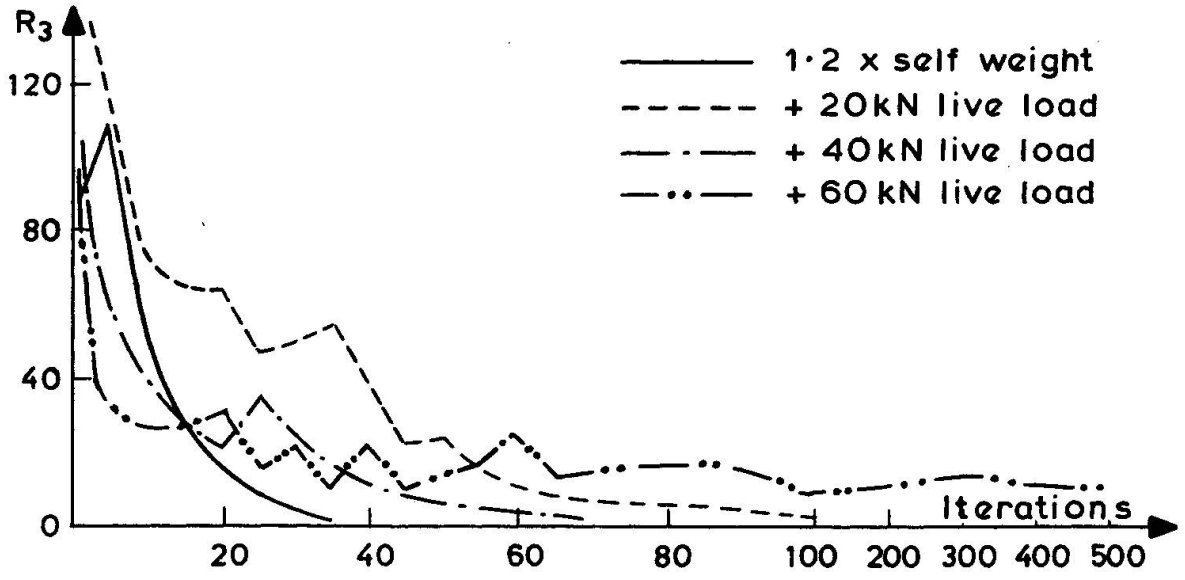

Fig. 3 Variation of R_3

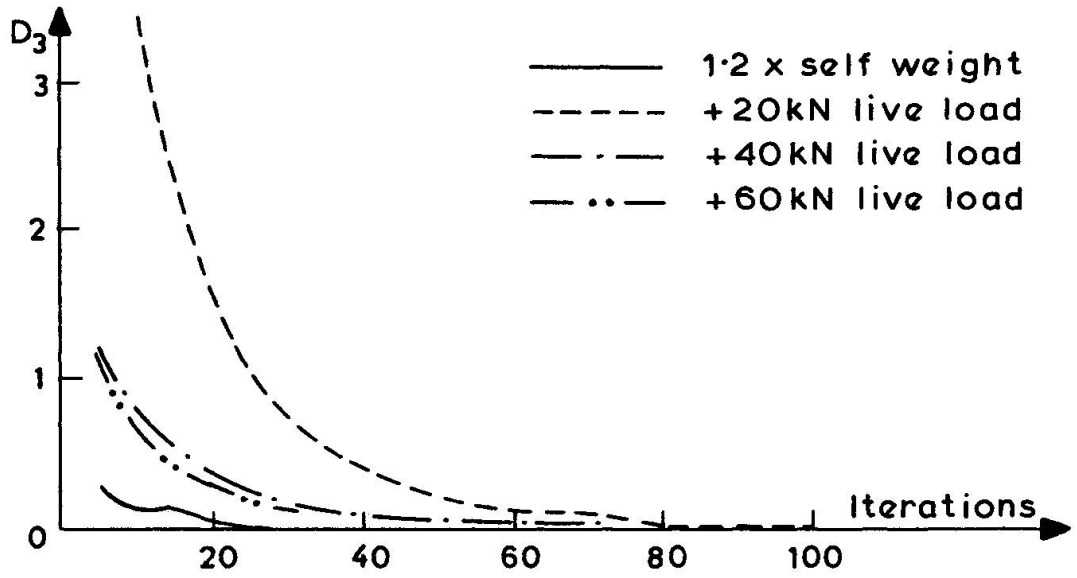

Fig. 4 Variation of D_3

The variations of the norms in the transverse direction (j = 3) are shown in Figs. 3 and 4. The high levels of R_3, at the start of iterations, indicates that most of the 'cracking' occurs on load application with substantial release of energy. At vehicle loads of 20kN and 40kN, although R_3 fluctuates, it ultimately reaches a small value. However, at 60kN, and for higher load increments, the norm R_3 tends to stabilise at a certain level, about 10% in this instance.

Examination of the force norms in other directions shows that they are still large, even when the transverse force norm R_3 has become small. Bergan and Holland [12] have noted that unbalanced loads can form self-equilibrating groups, with little influence on overall response, and a study of beams [8] has shown that the relative magnitudes of axial and couple norms are governed by the chosen shape functions. It thus seems unlikely that force norms will always converge to zero, even when a large number of iterations are performed. Bathe and Cimento [10] have observed that the modified Newton-Raphson procedure can diverge when out-of-balance forces increase during iterations.

As engineers are accustomed to relying on equilibrium checks, non-convergence of R_3 to zero is disquieting. However, engineers use linear harmonic analysis with confidence, and when a finite number of harmonics are used, there are sets of spurious self-equilibrating forces present and non-satisfaction of equilibrium norms. The analogy is a loose one, but as analytical results give satisfactory agreement with experimental values [6, 8] there is perhaps no cause for undue concern. Analyses of a wide range of slabs, in which out-of-balance forces fluctuated, gave acceptable results, and to the authors' knowledge, no divergent solution has been reported in the literature.

The transverse displacement norm D_3, which measures the rate of convergence, rather than absolute convergence, is shown in Fig. 4. Behaviour is less fluctuating with values approaching zero asymptotically.

3.2 Scaled Force and Displacement Norms

Chrisfield has recommended use of scaled norms [9] for terminating iterations. His norms are:

$$\bar{R}_j = \frac{\sqrt{\Sigma\ (\bar{P}_i - \bar{F}_i)^2}}{\text{Max}\left(\sqrt{\Sigma\ \bar{P}_i^{\,2}}, \sqrt{\Sigma\ \bar{r}_i^{\,2}}\right)} \tag{4}$$

and

$$\bar{D}_j = \frac{\sqrt{\Sigma\ \bar{\delta}_i^{\,2}}}{\sqrt{\Sigma\ \bar{U}_i^{\,2}}} \tag{5}$$

where $\bar{P}_i = P_i/\sqrt{K_{ii}}$ is the component of the nodal load in the j-direction, scaled by the reciprocal of the square root of the corresponding diagonal tangential stiffness coefficient at the beginning of the increment. The corresponding internally mobilised force F_i is scaled to give $\bar{F}_i$, and the $\bar{r}_i$ are similarly scaled reaction components at supported nodes. The displacement norm is obtained from $\bar{U}_i = \sqrt{K_{ii}}.U_i$ and $\bar{\delta}_i = \sqrt{K_{ii}}.\delta_i$, where U_i is the total accumulated displacement and δ_i is the displacement component obtained from the iteration. Analyses using limits of 10^{-4} on $\bar{R}_j$ and $\bar{D}_j$ to terminate iterations are referenced in [9].

Values of $\bar{R}_j$ and $\bar{D}_j$ for the analyses described in 3.1 are shown in Figs. 5, 6. On the whole, their behaviour is similar to that of the norms proposed by the authors. Similar fluctuations exist and there seems to be no advantage to compensate for the additional computing costs necessary to determine these norms. It should be stated that the tangential stiffness coefficients were determined using an arbitrary, small, positive value for concrete modulus at cracked integration stations. For the comparisons shown, a value of 0.05 times the uncracked concrete modulus was used.

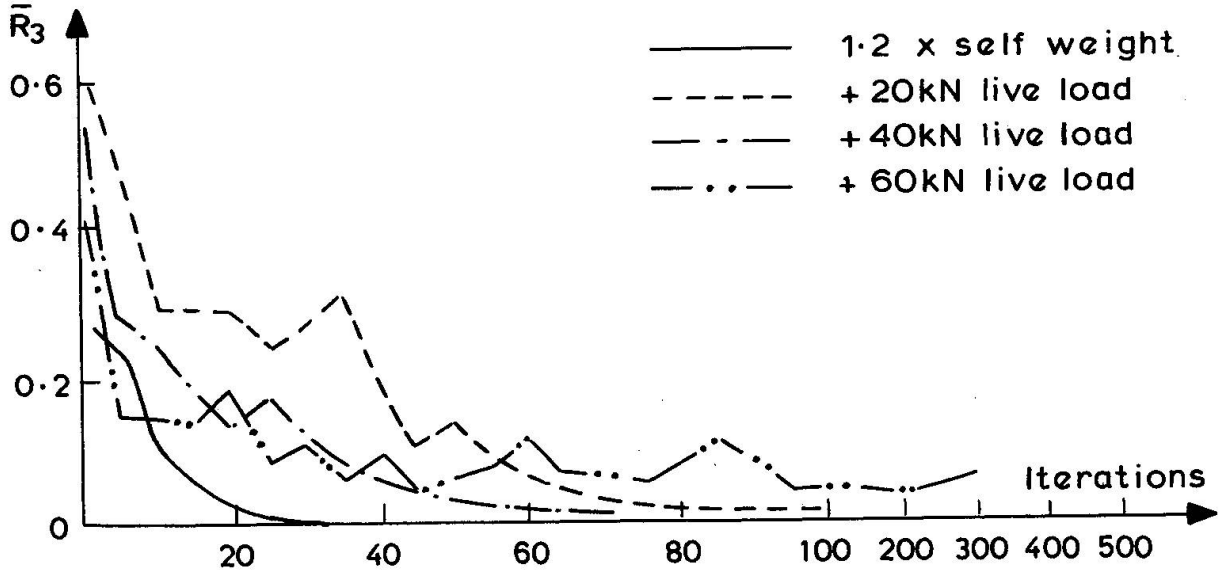

Fig. 5 Variation of $\bar{R}_3$

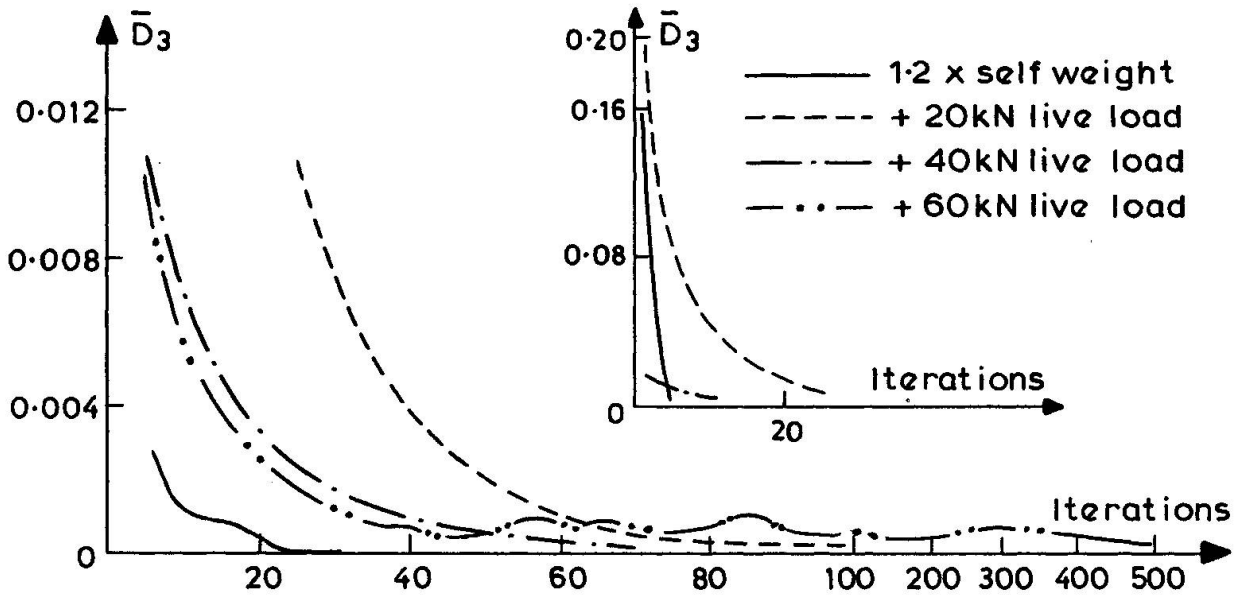

Fig. 6 Variation of $\bar{D}_3$

3.3 Energy Norms

Since both force and displacement monitoring is important, Bathe and Cimento [10] have recommended use of energy norms. The energy released during an iteration equals the work done, W, by the out-of-balance loads moving through the corresponding iterative displacements, thus:

$$W = \sum_j \sum_i (P_i - F_i).\delta_i \qquad (6)$$

Values of W with iterations, for the analyses described in 3.1, are given in Table 2. It is clear from these results that most of the energy release, prior to yielding of reinforcement, occurs during the first few iterations. This is consistent with other reported observations [3, 13].

Iteration	1	5	10	20	30	40	50	70	100	500
1.2 x Self Weight	2250	60	20	1	-	-	-	-	-	-
+ 20kN.	24000	15000	7500	2050	730	310	125	15	2	-
+ 40kN.	107000	2250	1200	300	210	60	20	2	-	-
+ 60kN.	8250	2250	1100	660	400	170	225	140	120	125

Table 2 Values of W with Iterations

The feasibility of using the ratio of energy released during an iteration to the maximum energy released in a previous iteration of that particular load increment has been studied [8]. A value varying between 0.01 and 0.025 gives acceptable results for the mesh size examined. The smaller value is used for the initial stages of intense cracking. Using such a norm results in solutions similar to those obtained using a limit of about 30 iterations, which is consistent with the results of 3.1.

3.4 Structural Integrity

To check structural integrity, strains can be monitored to assess crack widths, possible loss of ductility and extent of yielding. By studying the material damage predictions for a particular class of structure, experience can be gained and used as guides for designers. Since a numerical technique is being employed for analysis, a numerical measure is needed for any automated decision making.

Bergan [14] has advocated use of a current stiffness parameter, which attempts to express the stiffness at the current load level in terms of the initial linear stiffness. This parameter depends on the incremental load and displacement values. For the slab analysed above, it has the values 0.72, 0.09, 0.25 and 0.21 at 1.2 x self weight, and with live loads of 20kN, 40kN and 60kN, respectively, and the value 0.01 close to failure. Because the rate of stiffness degradation in concrete slabs is not uniform and decreases after first cracking, the parameter does not decrease monotonically. Also, before a single parameter could be used with confidence, experience is needed to see how it is affected by local as opposed to global failure.

An alternative indicator that could be used is the amount of energy being released due to structural damage, W. If the work done by the out-of-balance forces due to iterative displacements does not diminish or grows, there is a clear indication that the structure, or part of it, cannot sustain the applied loading.

4. ACCELERATION OF CONVERGENCE

From a study of numerical acceleration schemes [3,8], the recently implemented BFGS procedure [15] has been selected as the most efficient one available. Bathe and Cimento [10] have published results from studies of reinforced concrete beam behaviour and here, some of the effects of using the procedure to analyse slabs are presented. All of the numerical work reported was performed on a CDC 7600 computer using a constant stiffness matrix based on unstressed material properties.

4.1 Parameters STOL and CONDMAX

The two parameters of prime concern to users of the BFGS procedure are STOL and CONDMAX. STOL governs the number of line searches and iterations, and is set to a value between 0 and 1. It has been reported that as the value increases towards unity, although the number of line searches decreases, the number of iterations needed increases [15]. Analyses using STOL = 0.1 and 0.5 are presented. The decision to select a new search direction is taken by comparing the quadratic form of the stiffness matrix, with respect to the iterative displacement vector, with its previous value. This number is estimated and compared with the value of CONDMAX. It has been recommended that CONDMAX = 10^5, [15], leads to stable solutions. Here, results are presented for CONDMAX equal to 10^5 and 10^{10}.

4.2 Comparison of Solutions

Analysis of skew slab 2B of [8], with no tension stiffening, should provide a severe test of the method as it is the most flexible of the designs studied. Table 3 shows values of central deflection predicted and the numbers of iterations necessary to satisfy the prescribed norms. These were R_3 = 2% and D_3 = 0.02% for all analyses, with a maximum of 80 iterations performed in a load increment for an accelerated solution and 300 iterations for the solution without

acceleration. It can be seen that the use of the BFGS acceleration scheme reduced the number of iterations necessary to reach an equilibrium state, but for the two cases marked with an asterisk the procedure has converged to the wrong position. However, even in these two instances of unacceptable predictions, the procedure 'corrects' itself at higher load levels. This desirable feature occurs because internal forces are equilibrated to the total applied load.

Load	Without Acceleration	STOL = 0.1		STOL = 0.5	
		CONDMAX=10^5	CONDMAX=10^{10}	CONDMAX=10^5	CONDMAX=10^{10}
1.2xSelf Wt	1.3/ 31	1.3/13	6.3*/36	5.3*/34	1.3/ 9
+ 20kN	8.8/109	9.0/51	8.7 /29	8.5 /32	9.0/29
+40kN	11.4/ 72	11.5/27	11.5 /20	11.5 /30	11.5/25
+60kN	14.1/300	13.8/80	14.0 /80	13.9 /80	13.9/80

Table 3 Central Deflection/Number of Iterations

Further analyses to examine predicted response up to 20kN of live load are given in Table 4. In the analysis with no acceleration, the maximum energy release occurred during the sixth iteration of the 5kN load increment. From these results it is clear that considerable cracking occurs almost immediately and that the state of the slab at 1.2 times self weight is almost unstable. These results show that caution should be used if prediction of response during the initial phase of extensive cracking is required, but for most purposes there does not appear to be a serious problem.

Load	Without Acceleration	CONDMAX = 10^{10}	
		STOL = 0.5	STOL = 0.1
1.2 x Self Weight	1.33/ 31	1.31/ 9	6.26/36
+ 5kN	6.66/129	6.87/57	6.64/23
+ 10kN	7.14/ 53	7.30/19	7.30/16
+ 15kN	7.98/118	8.03/30	7.96/14
+ 20kN	8.70/ 64	8.68/14	8.69/20

Table 4 Central Deflection/Number of Iterations

A more detailed comparison of the predictions is given by examining the principal strains at the Gauss stations closest to the centre line. These are given in Table 5. In addition to the strains at 5kN increments values are presented for a single increment of 20kN. It can be seen that the results are in line with those for displacements. All of the predictions for the live load of 20kN lie within the accuracy that can be obtained from experiment [6] and there is no evidence to support preference for any particular set of values.

For further assessment of the overall influence of solutions following different load paths, the reactions under 1.2 times the self weight, plus a live load of 60kN, are given in Table 6.

It is clear from these results that convergence is not to a unique solution, but that there is an acceptable degree of agreement for design purposes. To examine the effects of limiting the number of iterations and of changing the size of the load increment to reduce costs of computation, further analyses were performed.

Load	Without Acceleration					
1.2 x Self Weight	173	181	186	184	167	154
+ 5kN	1315	1340	1387	1344	1291	1272
+ 10kN	1333	1409	1438	1397	1303	1308
+ 15kN	1498	1579	1568	1502	1383	1352
+ 20kN	1646	1736	1703	1615	1446	1427
+ 20kN direct	1798	1807	1756	1680	1560	1511
Load	STOL = 0.5 CONDMAX = 10^{10}					
1.2 x Self Weight	173	180	186	183	167	154
+ 5kN	1305	1351	1381	1349	1296	1285
+ 10kN	1328	1412	1454	1406	1292	1278
+ 15kN	1496	1566	1583	1509	1365	1335
+ 20kN	1617	1712	1719	1620	1460	1430
+ 20kN direct	1800	1789	1825	1650	1568	1521
Load	STOL = 0.1 CONDMAX = 10^{10}					
1.2 x Self Weight	1247	1227	1246	1248	1212	1159
+ 5kN	1201	1269	1318	1301	1203	1199
+ 10kN	1337	1415	1450	1409	1287	1284
+ 15kN	1478	1561	1592	1509	1372	1367
+ 20kN	1628	1717	1715	1623	1442	1426
+ 20kN direct	1626	1721	1711	1621	1435	1414

Table 5 Midspan Principal Strains

Without Acceleration	STOL = 0.1		STOL = 0.5	
	CONDMAX=10^5	CONDMAX=10^{10}	CONDMAX=10^5	CONDMAX=10^{10}
38.0	39.5	40.5	39.2	39.8
7.1	4.2	3.5	6.5	5.1
7.6	9.1	8.3	8.0	7.9
4.9	4.5	5.7	4.3	4.7
7.1	7.3	6.1	7.4	7.5
-0.2	-0.2	0.5	-0.4	-0.2

Table 6 Reactions at 1.2 x Self Weight + 60kN

In Table 7, values of central deflection are compared for 20kN load increments. The analysis using constant stiffness was conducted with norms of R_3 = 2% and D_3 = 0.05%, but with a limit of 300 iterations in any load increment. This latter criterion governed for the 60kN and subsequent increments. The accelerated analyses used STOL = 0.5 and CONDMAX = 10^{10}. Norms of R_3 = 2% and D_3 = 0.05% were set for these analyses, but with the maximum number of iterations in an increment as specified in the Table. Two further analyses were performed without acceleration and these were controlled by the energy norm. Iterations were stopped when the ratio of the energy norms W, (see Eqn. 6) reach 0.01 and 0.02, respectively.

Load	Without Acceleration	BFGS with Maximum Iterations			Without Acceleration Energy Control	
		10	40	150	0.02	0.01
1.2 x Self Wt	1.3	1.3	1.3	1.3	1.3	1.3
+ 20kN	8.8	8.8	9.0	9.0	8.2	8.5
+ 40kN	11.4	11.5	11.5	11.5	10.1	10.6
+ 60kN	14.1	13.9	13.9	13.9	13.7	13.9
+ 80kN	17.2	16.8	17.1	17.1	16.5	17.0
+ 100kN	21.4	21.3	21.5	21.5	20.9	21.0
+ 120kN	30.9	30.6	31.0	31.1	26.6	28.7
+ 140kN	48.2	45.9	49.3	49.2	45.0	47.0
+ 150kN	59.4		60.3	60.4		
+ 160kN	82.4		71.4			

Table 7 Central Displacement

Prior to extensive yielding of reinforcement, the BFGS solution using only 10 iterations per increment is acceptable. Results obtained using 40 and 150 iterations are virtually identical. After about 30 iterations the scaling factors from the line search procedure become very small and it appears that for most problems, with a constant stiffness approach, a maximum of 10 to 15 iterations per load increment should be adequate. No value is given for the BFGS solution with 150 iteration control at 160kN, as the allowable computer time had expired. At the stages of initial cracking, the analysis using the smaller energy ratio to control iterations is acceptable, and for high load levels both analyses gave similar results.

4.3 Cost of Solutions

Costs of solutions are compared in Table 8. The values given are based on computer mill time used. At 40kN, which corresponds approximately with the serviceability load level, the BFGS solution, with a limit of 10 iterations, costs only a quarter of the effort necessary for an analysis without acceleration. However, neither it, nor the solution using the energy norm, satisfied the limits set on the force and displacement norms. From the results given in Table 3, it can be seen that the BFGS solution, with a limit of 40 iterations, satisfied those norms, and that analysis halved the time of solution.

Load	Without Acceleration	BFGS Max Iterations		Without Acceleration
		10	40	0.01
1.2 x Self Weight	11.7	5.4	5.4	3.7
+ 20kN	53.8	12.4	24.0	21.5
+ 40kN	81.9	18.8	39.7	28.2
+ 60kN	196.9	25.1	74.9	53.4
+ 80kN	311.8	31.6	104.0	82.0
+ 100kN	426.7	37.9	135.8	115.6
+ 120kN	541.9	45.0	164.0	191.7
+ 140kN	657.1	51.3	189.6	268.0

Table 8 Cost Comparison

At higher load levels, none of the solutions satisfied the limits set on the norms, but the results from the analysis without acceleration and the solution using acceleration with the 40 iteration limit are similar. When the live load is at 80kN the cost of the accelerated solution is a third of that for the analysis without acceleration. This factor reduces slowly with increasing load level to approximately 0.3 at 140kN. But as even these analyses are expensive and results obtained with 10-15 iterations are reasonable those limits can be used for most purposes.

4.4 Size of Load Increment

A further way of reducing the costs of computation is to reduce the number of intermediate load increments. From the results given in Tables 4 and 5, it appears that deflections and strains in concrete slabs are relatively insensitive to the size of load increment. To assess the effect of load increment size, results of a number of analyses are compared in Table 9.

Load	Without Acceleration		BFGS	BFGS	BFGS
	(20kN)	(40kN)	(5kN)	(20kN)	(40kN)
1.2 x Self Wt	1.3	1.3	1.3	1.3	1.3
+ 20kN	8.8	-	8.7	8.8	-
+ 40kN	11.4	11.7	11.4	11.5	11.9
+ 60kN	14.1	-	13.9	13.9	-
+ 80kN	17.2	17.3	17.0	16.8	17.1
+ 100kN	21.4	-	21.5	21.3	-
+ 120kN	30.9	29.2	30.9	30.6	29.9
+ 140kN	48.2	47.5		46.0	46.5

Table 9 Central Displacement with Load Increment

To form a basis for comparison, the central displacements predicted by the analysis without acceleration, and with up to 300 iterations, are recorded. Results of three analyses from the BFGS solution with STOL = 0.5, CONDMAX = 10^{10}, and with a limit of 10 iterations per increment are presented. It can be seen that very similar predictions are obtained from all of the analyses. A comparison of strains and principal directions at mid-span has been made [8] which confirms that use of large load steps does not distort the response. This suggests that an engineer interested in effects at a particular load level could obtain those results with quite coarse load increments.

5. SHEAR

All of the skew slabs tested in an accompanying programme of experimental tests [6,8] showed severe inclined cracking in the obtuse corner region at high load levels. The plate element formulations used for the analyses reported above sets transverse shear strain to zero and hence cannot model this behaviour.

5.1 Heterosis Formulation

A study has been initiated to investigate the use of the Mindlin plate bending theory which accounts for shear strains. The 'heterosis' element [16] appears to be the best formulation and it has been implemented in its hierarchical form. 3x3 Gauss integration in plan has been used for both flexure and in-plane

effects. Material moduli are thus set on a 3x3x5 grid of sampling stations, in contrast to the more economical 2x2x5 grid used for the previous solutions. 2x2 integration stations are used for transverse shear, but for the preliminary results presented here, the rigidity modulus of concrete has been kept constant.

Analysis	Load							
	1.2xSelf Wt	+20kN	+40kN	+60kN	+80kN	+100kN	+120kN	+140kN
Previous	1.9	12.7	16.2	21.1	28.6	40.0	62.7	96.6
Heterosis	7.9	11.6	16.8	21.6	29.3	39.9	59.3	99.1
ER = 0.01	7.6/51	10.0/11	16.4/36	21.3/41	28.8/51	38.5/51	57.4/131	98.8/241
ER = 0.02	7.5/46	9.5/ 6	16.2/26	21.2/36	28.6/46	37.6/36	54.8/76	97.4/211

Table 10 Maximum Displacement Comparison

In Table 10 values of maximum displacement for skew slab 2B are compared with results from the previous analysis. Because of the sensitivity of this particular slab to perturbations under self weight, the change in shape functions has triggered off additional cracking. However, at later load levels, the response is similar to that obtained from the previous analysis.

The work done by the out-of-balance loads is computed using only in-plane and rotational displacements, since with a constant shear modulus this formulation does not produce any transverse out-of-balance forces. The norm R_3 cannot, therefore, be used to monitor convergence. To assess the possibility of using the energy norm W to control the number of iterations, values are also presented for energy ratios, ER, of 0.01 and 0.02 (ER = energy released in current iteration divided by maximum released energy in an iteration of the load increment). The number of iterations is also presented as a guide to the relative costs of these analyses.

6. CONCLUSIONS

Application of non-linear numerical techniques to concrete structures is complicated by the lack of uniformity in stiffness degradation and by the different load-unload paths. These features make it particularly difficult to specify norms to automatically control the number of iterations to be performed. It is clear from the results of this study that no single, unambiguous and precise measure exists, and that judgement is needed to assess the results of non-linear analyses of concrete slabs.

For design of slabs, a uniaxial stress-strain relationship can be used for concrete and tension stiffening effects need not be simulated. Analyses in which orthotropic material property axes are not fixed in directions dictated by initial cracking give better comparisons with experimental results than those in which 'crack' directions are fixed. Acceptable results can be obtained using the BFGS acceleration procedure and relatively coarse load increments to reduce the cost of analysis.

In skew slabs there is a need to implement formulations which do not employ Kirchhoff's restraints. The heterosis finite element formulation of the Mindlin plate theory promises to be a suitable approach and further studies are being undertaken to examine the possibility of incorporating the effects of inclined cracking.

REFERENCES

1. BS5400 for the Design of Steel, Concrete and Composite Bridges, London, 1978.

2. Baldwin, J. T., Razzaque, A., Irons, B. M. 'Shape Function Routine for an Isoparametric Thin Plate Element', Int. Jnl. for Num. Meth. in Eng'g, V7, 1973.

3. Cope, R. J., Rao, P. V., Clark, L. A. 'Nonlinear Design of Concrete Bridge Slabs using Finite Element Procedures', Nonlinear Design of Concrete Structures, Univ. of Waterloo, 1980.

4. Cope, R. J., Rao, P. V., Clark, L. A., Norris, P. 'Modelling of Reinforced Concrete Behaviour for Finite Element Analysis of Bridge Slabs', Numerical Methods for Nonlinear Problems, V1, Pineridge Press, 1980.

5. Gilbert, R. I., Warner, R. F. 'Tension Stiffening in Reinforced Concrete Slabs', Proc. ASCE, V104, ST12, 1978.

6. Cope, R. J., Rao, P. V. 'Reinforced Concrete Skewed Bridge Slabs', Advanced Mechanics of Reinforced Concrete, IABSE Colloquium, Delft, 1981.

7. Bažant, Z. P. 'Advances in Deformation and Failure Models for Concrete', IABSE Colloquium, Delft, 1981.

8. Cope, R. J., Rao, P. V. 'Behaviour of Reinforced Concrete Bridge Slabs', Technical Report, Dept. Civil Eng'g, Univ. of Liverpool, 1981.

9. Chrisfield, M. A. 'A Faster Modified Newton-Raphson Iteration', Computer Methods in App. Mechs. and Eng'g, 20, 1979.

10. Bathe, K. J. and Cimento, A. P. 'Some Practical Procedures for the Solution of Nonlinear Finite Element Equations', Computer Methods in App. Mechs. and Eng'g, 22, 1980.

11. Cope, R. J., Rao, P. V., Edwards, K. 'Nonlinear Finite Element Analysis Techniques for Concrete Slabs', Numerical Methods for Nonlinear Problems, V1, Pineridge Press, 1980.

12. Bergan, P. G., Holland, I. 'Nonlinear Finite Element Analysis of Concrete Structures', Computer Methods in App. Mechs. and Eng'g, V17/18, 1979.

13. Cedolin, L., Nilson, A. H. 'A Convergence Study of Iterative Methods applied to Finite Element Analysis of Reinforced Concrete', Int. Jnl. for Num. Methods in Eng'g, V12, 1978.

14. Bergan, P. G., Holland, I., Söreide, T. H. 'Use of Current Stiffness Parameter in Solution of Nonlinear Problems', Energy Methods in Finite Element Analysis, J. Wiley & Sons, 1979.

15. Matthies, H., Strang, G. 'The Solution of Nonlinear Finite Element Equations', Int. Jnl. for Num. Methods in Eng'g, V14, 1979.

16. Hughes, T. J. R., Cohen, M. 'The "Heterosis" Finite Element for Plate Bending', Computers and Structures, V9, 1978.